Int. J. of Applied Mechanics and Engineering, 2006, vol.11, No.3, pp.479-490

This paper was prepared on the Fourth International Tribology Conference ITC 2006

DEVELOPMENT OF A METHOD FOR THE ANALYSIS OF MIXED FRICTION PROBLEMS

A. ALBERS, L. NOWICKI* and H.-G. ENKLER
IPEK, Institute of Product Development, University of Karlsruhe
Kaiserstr. 12, 76128 Karlsruhe, GERMANY
e-mail: nowicki@ipek.uni-karlsruhe.de

This article deals with a holistic approach to the numerical analysis of mixed friction. By means of the finite element method, the influence of a set of selected parameters on the behaviour of the frictional contact system will be determined. To this end, a three-dimensional parameterized FEM-model will be presented, which couples the equations of the structure mechanics with the Navier-Stokes-theory. To consider the roughness of machined surfaces, virtual surfaces are generated to represent the characteristics of usual manufacturing methods. At the Institute of Product Development, the theoretical approaches were implemented into a software code, which makes use of stochastic algorithms to obtain rough surfaces with the desired characteristics. The characterization of these virtual surfaces is done by the abbot curve and a roughness parameter. The generation of the surfaces is done by an evolutionary optimizer.

Key words: FEM, FSI, mixed friction, surface roughness, tribology.

1. Preface

Frictional contacts are part of almost any technical system. They are of vital importance for the reliability of such a product. The functional adequate design of the contact surfaces requires the development of a method that allows studying friction mechanisms of the tribological system. Due to the continuous development of computer technology, numerical simulations take center stage. Today it is possible to represent reality with models that have a high level of detail. Thus new fields of application for the CAD engineers are offered. By means of three-dimensional models complex flow conditions can be investigated. The coupling of the structural mechanics and the world of fluids is no longer an insuperable technical challenge. Because of this the Institute of Product Development (Karlsruhe) developed an approach that permits the calculation of lubricated friction problems. In the beginning of the research the demands on the developing methods were defined:

- **Completely virtual process**
  Continuous integration of all the analysis methods applied should be guaranteed. The simulation should show an automated cycle.
- **Integration of standard software**
  Due to the application of commercial and free calculation tools the know-how of specialists of other disciplines like informatics or mathematics should be made accessible. The work should focus on the reflection of the reality of a fluid mechanic model. This at the same time increases the chances for an industrial application.
- **Adaptability for tasks like in real applications**
  This method should transcendent academic examples. The calculation of complex and close to industry problems should be guaranteed. A three-dimensional stream simulation with respect to the topography of real technical surfaces shall be made possible.

* To whom correspondence should be addressed

The design of the complete virtual process is shown in Fig.1. In order to solve the problem a macro model is created and calculated. In this model the influence of the surface roughness is not considered, i.e., it is assumed that the bodies are perfectly smooth. With these modes by tribological means critical areas like the minimum crack size and the location of the greatest pressure are detected. These critical locations are reconsidered using the micro model. Therefore, the results of the macro world (distribution of compression in the fluid and its velocity profile) are used as boundary conditions. The influence of the surface roughness is taken into account by impressing a given topography onto the solid bodies. A static calculation of the micro model is preceded in order to get meaningful initial values for the transient analysis.

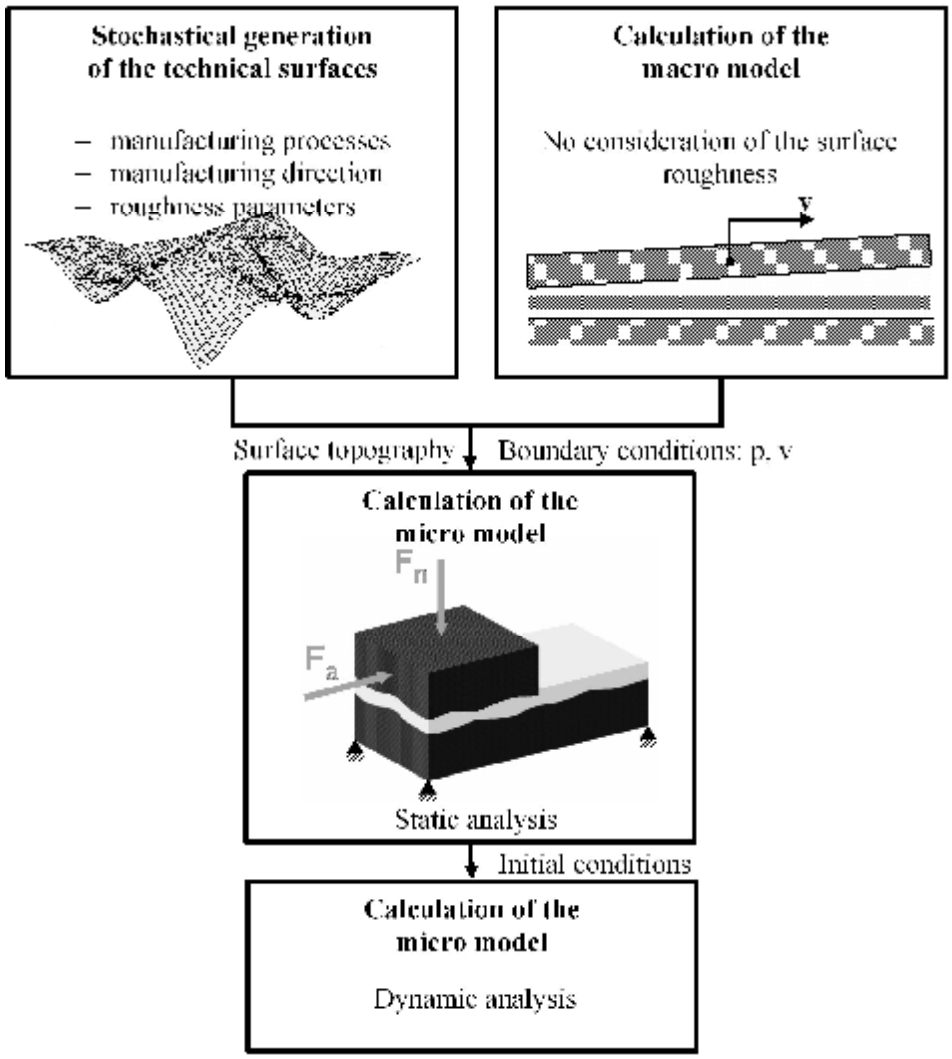

Fig.1. Flow chart of the overall process.

2. Generating of virtual machined surfaces

The challenge during the description of the surface characteristic is the allocation of a numerical value to surface, which describes its substantial characteristics and supplies expressive data concerning its function behaviour (Rometsch and Letzner, 1993). For a complete description of the surface properties the

shape of the profile must be taken into account exceeding the well-known arithmetic (R_a) and square (R_q) roughness factors or the averaged depth of roughness $(R_{z(DIN)})$. This happens by dint of the linear material ratio curve (Abbott curve), which illustrates the increase of the material load share (M) as a function of the increasing depth of profile (R) of the rough surface. It can be divided into three sections by means of three parameters: reduced peak height (R_{pk}), reduced valley depth (R_{vk}) and core roughness depth (R_k) DIN EN ISO 13565 (1997). The core roughness depth describes the area of the profile which shows the highest increase of the material load share. The reduced peak height gives the shape and the number of the roughness amplitudes. Analogously, the R_{vk} parameter describes the valley section. The sum of these three parameters constitutes the maximum height of the profile (R_t).

Figure 2 shows two surfaces of the same arithmetic mean value as well as profile height but with different profile characteristics. The upper surface has a relatively high roughness amplitude section and a small valley depth section. For contact examination this means that the multitude of peaks only guaranties a small nominal contact area, which results in high contact friction and heat. The lower surface, however, has a rather small roughness amplitude section but a larger valley depth section. Therefore, the nominal contact area is bigger. Also, in lubricated contacts grease pockets can occur in the valley depth section, which, for instance, allows a better drawing off heat.

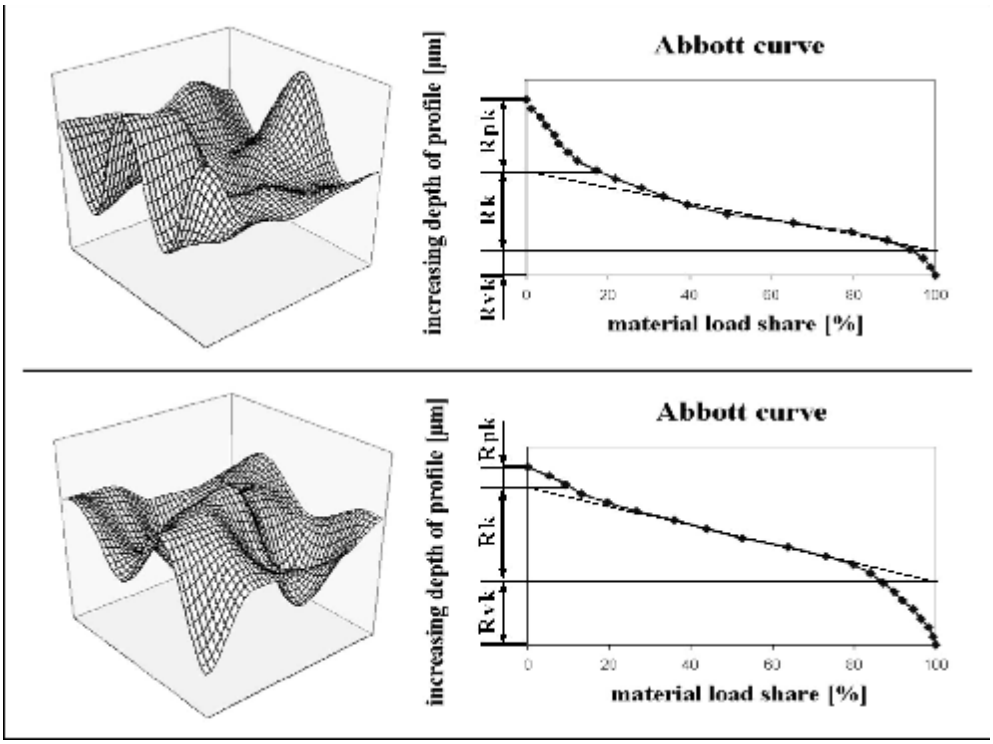

Fig.2. Stochastically generated surfaces

upper: $R_a = 0.4$, $R_t = 2.7$, $R_{pk} = 1.12$, $R_k = 1.23$, $R_{vk} = 0.35$

lower: $R_a = 0.4$, $R_t = 2.7$, $R_{pk} = 0.37$, $R_k = 1.43$, $R_{vk} = 0.96$

For further procedures it is necessary to determine quantifiable parameters for the surface characterization. For the description of the Abbott curve, the material load share (M) is regarded as the function of the depth of profile (R).

$$M = f(R). \tag{2.1}$$

Using the above, vector $\boldsymbol{A}$ of the following kind can be formed

$$\mathbf{A} = \left\{ \begin{array}{c} M_0 = M(Rt) \\ M_1 = M\left(\frac{n-1}{n} Rt\right) \\ M_2 = M\left(\frac{n-2}{n} Rt\right) \\ . \\ . \\ . \\ M_n = M(0) \end{array} \right\}, \qquad n = 20. \tag{2.2}$$

For the description of the surface roughness, the root mean square (R_q) is used. However, the procedure introduced here can also be transferred to the other roughness parameters.

2.1. Mathematical description of surfaces

A particular demand on the mathematical description method of technical surfaces is its applicability to several manufacturing processes. This requirement excludes the use of polynomials of a constant order since it changes depending on the manufacturing processes. Polynomials describing lapped surfaces would be of a much higher order than polynomials describing lathe surfaces. To solve this task, harmonic functions are used instead of polynomials. The Discrete Fourier Transformation (DFT) can be used in the most common manufacturing processes.

For the analysis and synthesis of technical surfaces, a two-dimensional transformation based on the following equations (Sundararajan, 2001) must be carried out

$$Z(\omega_1, \omega_2) = \sum_{x=0}^{N-1} \sum_{y=0}^{N-1} z(x, y) e^{-j\omega_1 \frac{2\pi x}{L}} e^{-j\omega_2 \frac{2\pi y}{L}}, \quad \omega_1, \omega_2 = 0,1,..., N-1, \tag{2.3}$$

$$z(x, y) = \sum_{\omega_1=0}^{N-1} \sum_{\omega_2=0}^{N-1} Z(\omega_1, \omega_2) e^{j\omega_1 \frac{2\pi x}{L}} e^{j\omega_2 \frac{2\pi y}{L}}, \quad x, y = 0,1,...,N-1. \tag{2.4}$$

The examined surfaces have the dimensions $500\mu m \times 500\mu m$ (sample rate $2\mu m$) and have been manufactured as follows:

- Milling (R_q: $2.83\mu m$, $0.58\mu m$)
- Turning (R_q: $4.25\mu m$, $1.03\mu m$)
- Grinding (R_q: $0.67\mu m$, $0.35\mu m$)
- Lapping (R_q: $0.52\mu m$, $0.21\mu m$)

For each surface, the frequency spectrum with its corresponding amplitudes, the Abbott curve, as well as the R_q-value were determined. The examination focused on how many of the approximately *31000* amplitudes play a significant role. For this, in case 1 all amplitudes were counted which were more than *15%* of the highest value. In other cases the bound was reduced to *10%* (case 2) and to *5%* (case 3).

Figure 3 shows the analysis results of a turned surface turning $(R_q = 1.03\mu m)$ as well as the dominant amplitudes of case 1. The example reflects very well the trend of the whole examination. All surfaces can be described by a manageable amount of frequencies. All significant amplitudes were in the first five columns and rows of the Fourier matrix. Manufacturing processes with geometric definite cutting edge showed less dominant amplitudes than manufacturing processes with geometric indefinite cutting edge. The number of amplitudes depended very much on the roughness value. With decreasing R_q-values, more high-frequency components occurred. In case 1 the number of relevant amplitudes depending on the manufacturing process was between 11-28 amplitudes. In case 2 this range increased to 17-54 amplitudes and in case 3 to 32-198 amplitudes. In order to examine in how far it is allowed to neglect the remaining frequency components, a reverse transform with solely the dominant amplitudes was carried out in all three cases and the reversely transformed surfaces were compared with the original versions. Already in case 1, the reduced surfaces showed characteristics similar to the measured surfaces. This allowed the conclusion that surfaces with desired characteristics can be generated with a small number of amplitudes.

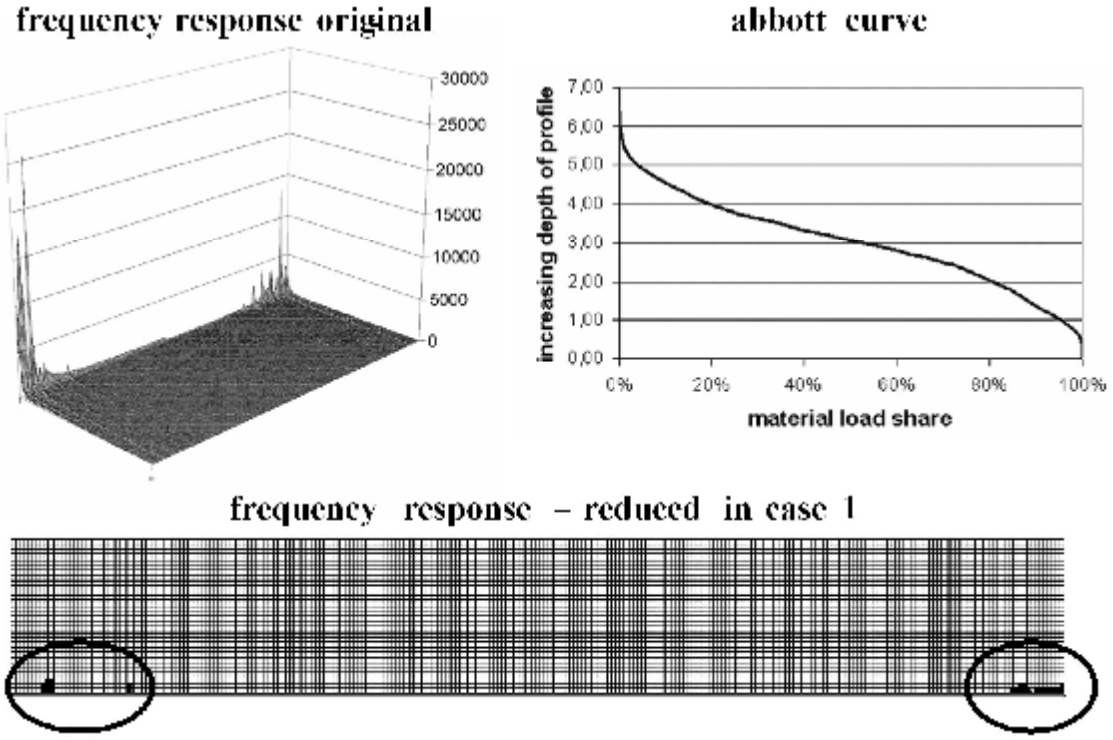

Fig.3. Frequency spectrum and abbott curve of measured turned surface $(R_q = 1.03\mu m)$, number of dominant amplitudes: *18*.

2.2. Evolutionary algorithms

For generating the technical surface with a given characteristic, an optimization algorithm was chosen, which is based on the biological process of evolution. This optimization algorithm was developed in Germany at the beginning of the seventies (Kursawe and Schwefel, 1997; Rechenberg, 1973; Albers *et al*., 2005) and is nowadays established as a standard tool for optimization. It is used for problems with a huge area of design and is highly nonlinear with lots of local extremes. Searching for the optimum is done by generating multiple, stochastically distributed points in the design area – called individuals - weighting them

with respect to the value of the objective function. Based on the individuals with the best fitness, a new group – called generation – is created. This process is repeated iteratively until an optimum is reached.

Based on Eqs (2.2) and (2.4), the following objective function is defined

$$f(z, \boldsymbol{A}_{Pattern}) = \boldsymbol{A}(z) \bullet \boldsymbol{A}_{Pattern}.$$

Based on that the following formulation for the optimization problem is defined

$$\begin{aligned} &\text{Maximize} \quad f(z, \boldsymbol{A}_{Pattern}) \\ &\text{Subject to} \quad h(z) = R_{q\_constraint} \end{aligned} \tag{2.6}$$

This means that the scalar product of vector $\boldsymbol{A}$ for the generated surface and vector $\boldsymbol{A}$ for the measured surface should be maximized with the restriction that the value for $R_{q\_constraint}$ must correspond to the given value.

2.3. Results of the surface generation

Two optimization tasks were set up for the manufacturing process ”turning” in order to verify the method. For both optimizations the abbot curve from Fig.3 was used for reference. The constraint in optimization 1 was a value of $1.5\mu m$ for R_q and a value of $2.5\mu m$ for R_q in optimization 2.

Figure 4 shows the stochastically generated surfaces. You can see the characteristic topographies of the turned surfaces. The scalar product of the vector $\boldsymbol{A}$ for the first result with vector $\boldsymbol{A}$ for the reference surface yields a value of *0.9999* which means that the characteristic of both abbot curves is very similar. The equality constraint could be preserved very well with a value of $1.5005\mu m$ for R_q. The quality of the second result is less accurate than the first one but still good enough. The scalar product of the vectors is *0.9947* and the value of R_q is $2.4959\mu m$.

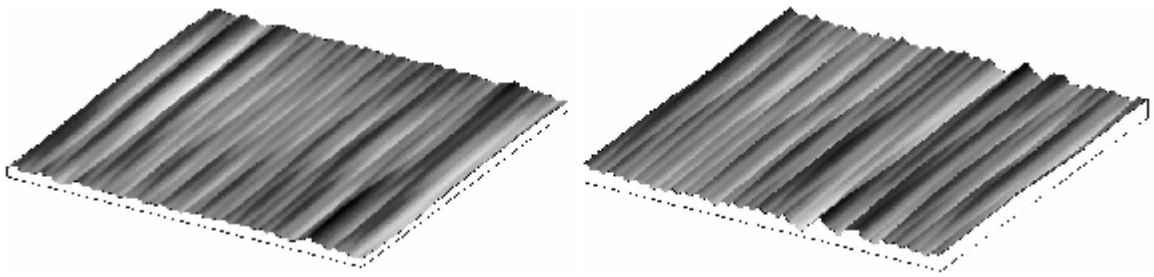

Fig.4. Stochastic generated surfaces left: $R_q = 1.5\mu m$, right: $R_q = 2.49\mu m$.

3. Finite element model for the numerical analysis of mixed friction

The micro model shown in Fig.5 consists of two three-dimensional rough solid bodies which are in contact. There is a fluid between the two solid bodies. The nodes of the lower body are fixed in order to guarantee static determinations. The upper body is gliding over the lower body and the fluid. The guiding can take place by forced displacement or force transmission. In order to describe the ratios in the fluid the Navier-Stokes equation is set up and solved numerically. The fluid is a non Newtonian fluid. The relation between the stress tensor and the shear rate follows the exponential law

$$\tau = k\left|\dot{\gamma}\right|^{n}\dot{\gamma}\;\forall\left(n<0\right), \tag{3.1}$$

with: τ = stress tensor, $\dot{\gamma}$ = shear rate, k = material constant,
n = degree of the power arrangement

The dependence of the viscosity on pressure and temperature can be considered but it has not been considered in this work. The interaction between the upper body and the fluid has been left beside since it is a boundary condition. The number and type of boundary conditions depend on the defined problem.

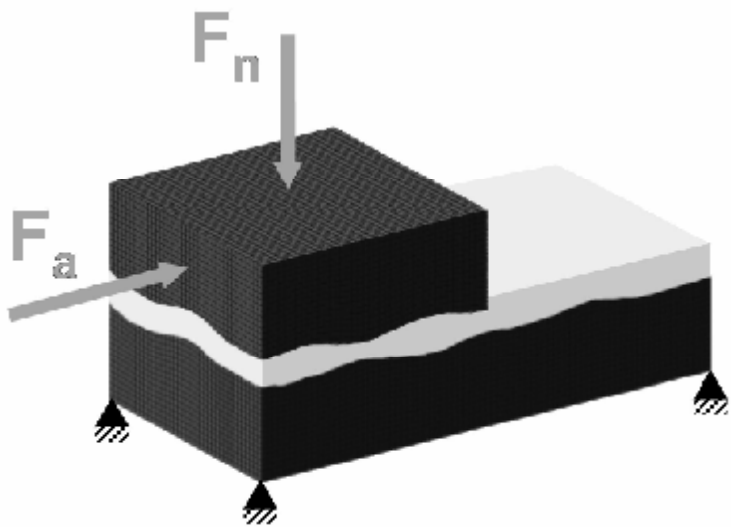

Fig.5. Micro model.

3.1. Preprocessing

For the numerical analysis of mixed friction two independent models need to be created. One model reflects the world of structural mechanics, the other model reflects the fluid mechanics. The approach of the creation of both models is similar. Therefore the process is explained using the fluid model (Fig.6).

– **Read in the virtual surfaces**
  Measuring or generated points on both surfaces are collected and sorted according to their coordinates. It is presupposed that each point is equidistant
– **Detection of contact points**
  Contact areas are determined for both surfaces. If there are two points on both surfaces closer than a given limiting value they come together. In the fluid model, the points are removed. In the body model, the contact boundary conditions are defined.
– **Creation of the geometry**
  By using the given points the following equation for the upper and lower surface can be build:

$$z\left(x,y\right)=Ax+By+Cxy+D \tag{3.2}$$

where *A, B, C, D* are constant.
The other surfaces are plane.

– **Meshing the models and adding the boundary conditions**
First of all, the model is meshed with 2-dimensional elements. Then with the aid of the *2-d* mesh a *3d* mesh with tetraeder is generated. These are elements of linear approximation. Node- and element-face groups are builtup. With them all necessary boundary conditions can be defined.

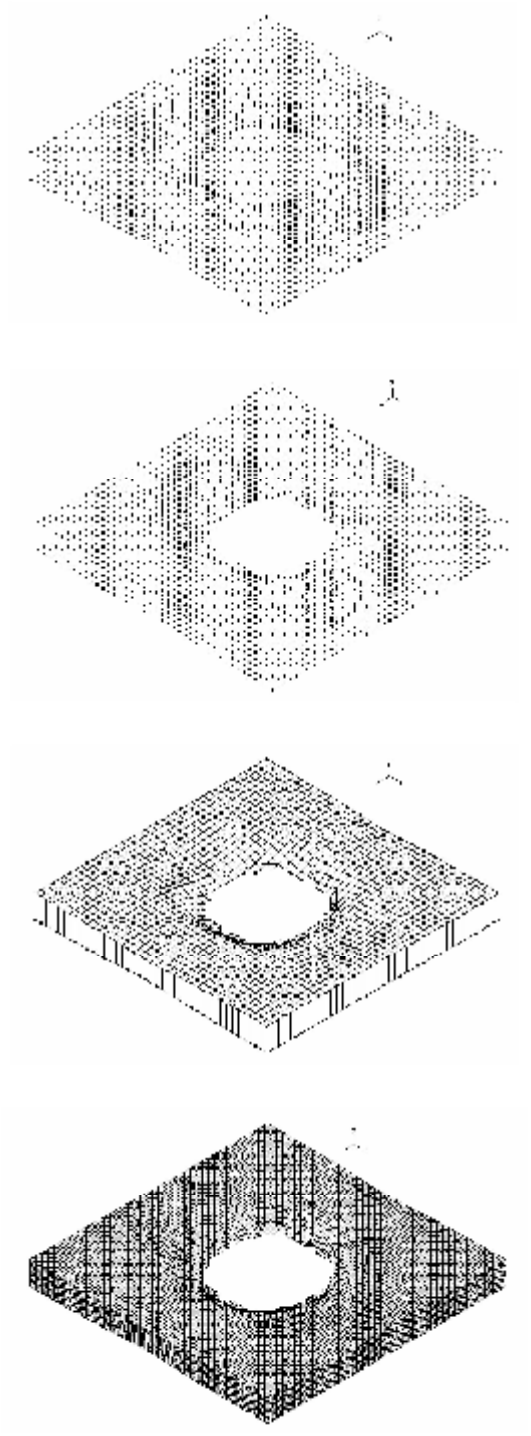

Fig.6. Preprocessing of the fluid model.

3.2. Controlling of the transient solution

During the transient analysis the upper body glides on the lower. This causes two important effects. On the one hand, new contact points are created during the analysis, causing a penetration of the fluid in between. On the other hand, the mesh of the fluid is deforming during the gliding. In order to avoid this, both models are remeshed all the time. After each successful step (see Fig.7) the areas of the net that show the rough surfaces are being separated. Then two new point lattices are generated in these areas. With these point lattices the preprocessing can be repeated. The results of the last step are mapped in the new interlaced model. This strategy requires two important criteria. The steps in the analysis need to be small and the grid fine enough. If the steps are too big a new contact point can occur and the net can be overtopped. If the chosen lattice spacing is too big, the topography of the surface can change due to the overtopping.

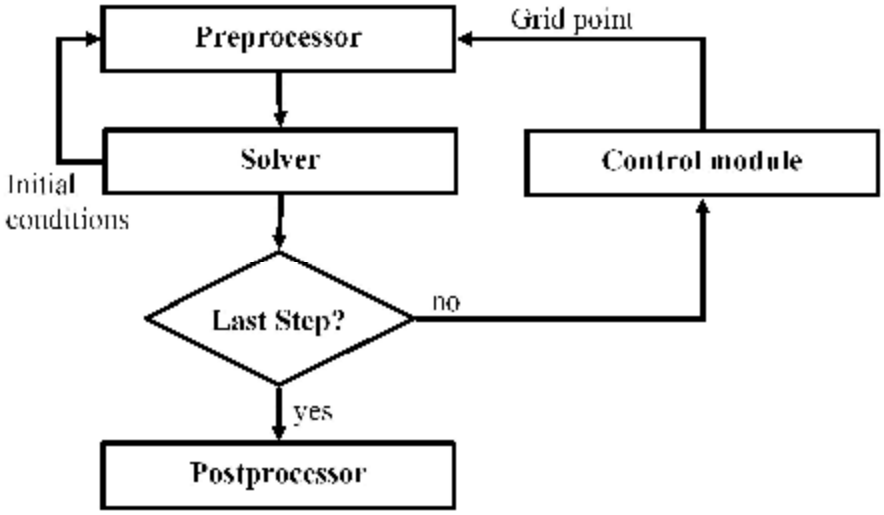

Fig.7. Solution process.

3.3. Example

The method will be exemplified with an axial friction bearing. Figure 8 shows a typical configuration of such an axial friction bearing. At a distance of a few micrometers a beveled shoe slides over the sliding surface.

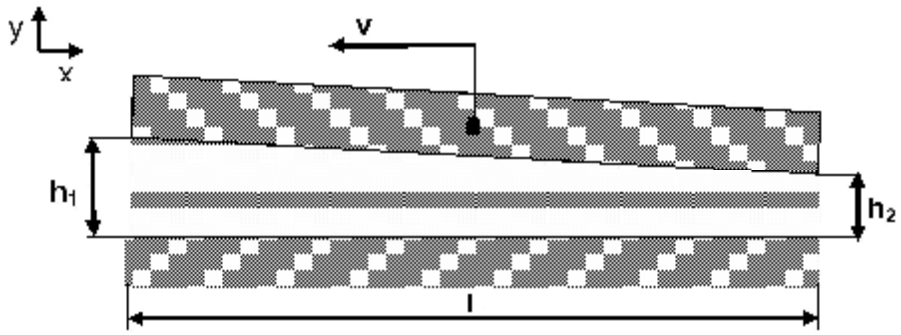

Fig.8. Axial friction bearing.

The size of the crack can be described by a linear function

$$h(x) = h_1 - \frac{h_1 - h_2}{L} x. \tag{3.3}$$

Due to the sliding movement of the shoe the oil is pressed into the beveled crack. This causes a rise in pressure, which prevents mechanical contact of the shoe and the sliding surface. Inside of the crack the pressure distribution can be obtained as follows

$$p(x) = \int_0^L 6\eta v \left(\frac{1}{h^2(x)} + \frac{c_1}{h^3(x)} \right) dx, \tag{3.4}$$

with: η = viscosity, v = velocity, c_1 = constant.

In this example, a maximum crack size of $9\mu m$ and a minimum crack size of $5\mu m$ are assumed. The length of the shoe is $100\ mm$ and its velocity is $600\,mm/s$, while the oil's viscosity is $2.2e-8\,Ns/mm^2$. Figure 9 shows the pressure distribution within the crack. The pressure takes a maximum value of $23.9\,bar$. At this location, the crack's size is $6.5\mu m$. In what follows a calculation with the micro model will be made.

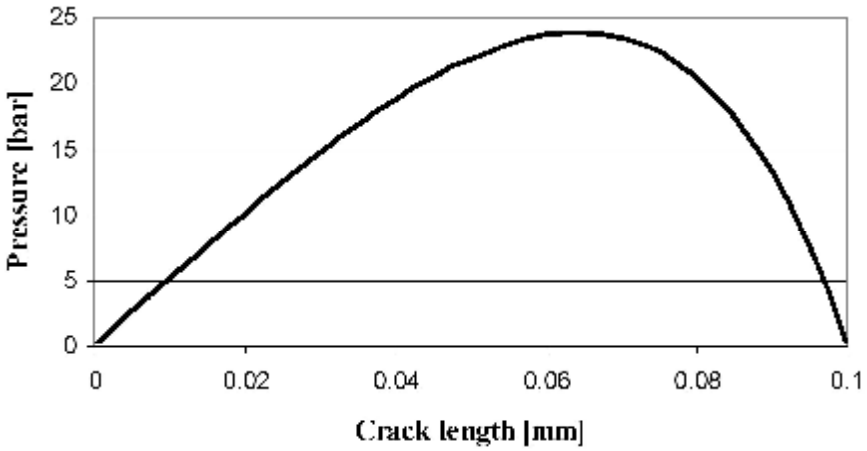

Fig.9. Pressure distribution in the crack.

Besides the boundary conditions from the macro model, additional information of the surface's topography is required for developing the micro model as shown in Fig.1. In this example, a measured surface is used. It is a ground surface with an arithmetic mean of $0.09\mu m$. From this surface two areas have been chosen for the micro model. They are shown in Fig.10. An area of $50\times50\mu m$ has been separated for representing the shoe, while the sliding surface is represented by an area of $75\times50\mu m$. The topography shows a certain kind of defect which will lead to a penetration of the oil in the course of the calculation.

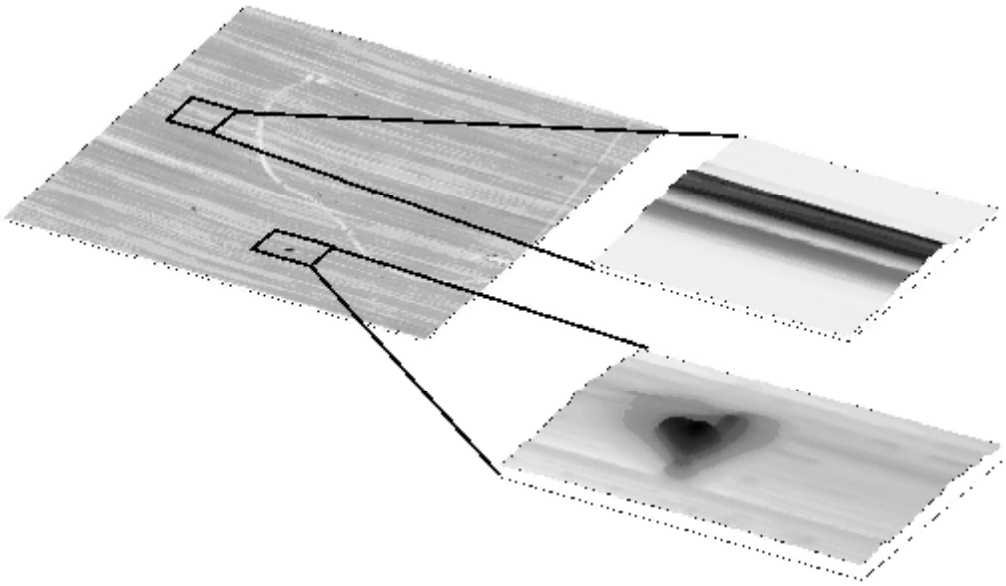

Fig.10. Surface roughness left: measured surface, right: parts of the FE-model.

The distance of the midplanes of both solids is set to $6.5\mu m$ by a constraint (Fig.11, left). On both solids a contact boundary condition has been set (Fig.11, right). Furthermore, an interaction between the fluid and the solid has been defined. The solid model shows a linear material behavior and consists of *300,000 degrees* of freedom. The flow is assumed to be laminar. The number of degrees of freedom is *35,000*.

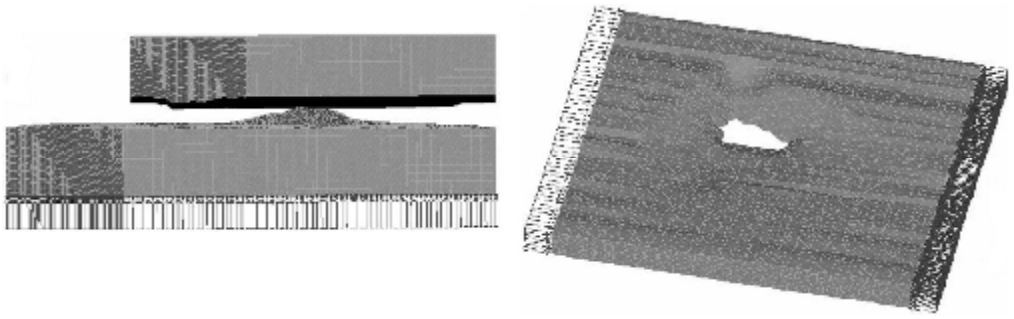

Fig.11. FE-model axial friction bearing left: solids, right: fluid.

Figure 12 shows an extract of the static analysis results. The pressure distribution within the fluid is described by the greyscales. The fluid flows from the left to the right with the preset velocity. As expected, the decrease of the crack's size and the direction change lead to an increasing pressure at the left before the penetration of the fluid. Vacuum forms at the right side. A further noticeable area can be found below the hole. As before, the pressure change is due to the variation of the crack's size.

The example shows that the roughness of the surface may cause local pressure fluctuations. Here, the rise in pressure compared to the value from the macro model is rather minor, so the influence of the fluid's pressure on the deformation of the solids can be neglected. But in the case of high sliding velocities and high gradients in the crack's size due to the surface's roughness, an elastohydrodynamic state with pressures of several thousand bar is reached. Then local effects affect stiffness and friction coefficient. These effects can be analyzed with the approach described here.

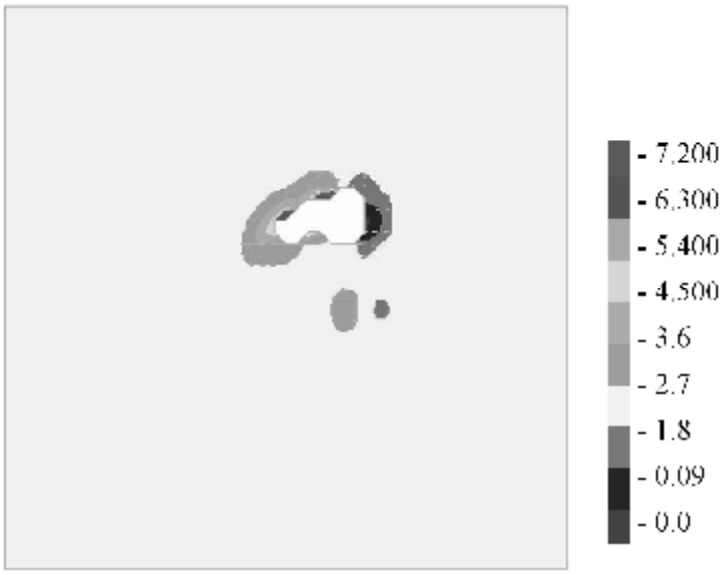

Fig.12. Pressure distribution in the fluid.

4. Conclusion

The approach introduced in this article permits a calculation of lubricated friction contact in the field of mixed friction using commercial and free software tools. The stochastic surfaces are created by using the Fourier-transformation and the stochastic algorithm for optimization. The calculation of mixed lubrication is made using the finite element method. Due to this the approach permits the investigation of the physical mechanisms of lubricated friction contact. The method has been exemplified with an axial friction bearing.

References

Albers A., Nowicki L. and Minx J. (2005): *A method for the consideration of influences of the surface roughness on the behaviour and design of global systems*. – 15th International Conference on Engineering Design ICED 05, Melbourne, Australia, August 15th -18th.

DIN EN ISO 13565 (1997): *Oberflächenbeschaffenheit: Tastschnittverfahren*. – Part 1 till Part 3. Hrsg, Deutsches Institut für Normung. Berlin, Köln: Beuth-Verlag.

Kursawe F. and Schwefel H-P. (1997): *Optimierung mit Evolutionären Algorithmen*. – Automatisierungstechnische Praxis, vol.39 No.9, pp.10-17.

Rechenberg I. (1973): *Evolutionsstrategie: Optimierung technischer Systeme nach Prinzipien der biologischen Evolution*. – Stuttgart: Frommann-Holzboog.

Rometsch R. and Letzner R-D. (1993): *Rauheitsmessung, Theorie und Praxis*. – Hommelwerke GmbH, Schnurr Druck.

Sundararajan D. (2001): *The Discrete Fourier Transform*. – World Scientific Publishing Co. Pte. Ltd., Singapore, New Jersey, London, Hong Kong.

Received: May 29, 2006
Revised: June 30, 2006